TECHNICAL ARTICLE

Potassium-ion intercalation in graphite within a potassium-ion battery examined using *in situ* X-ray diffraction

James C. Pramudita,[1,2] Vanessa K. Peterson,[2,3,a)] Justin A. Kimpton,[4] and Neeraj Sharma[1]
[1]*School of Chemistry, UNSW Australia, Sydney NSW 2052, Australia*
[2]*Australia Nuclear Science and Technology Organisation, Kirrawee, DC NSW 2253, Australia*
[3]*Institute for Superconducting and Electronic Materials, Faculty of Engineering, School of Mechanical, Materials, and Mechatronic Engineering, University of Wollongong, NSW 2522, Australia*
[4]*Australian Synchrotron, 800 Blackburn Road Clayton, VIC 3168, Australia*

(Received 28 April 2017; accepted 25 July 2017)

Graphite has been widely used as a negative electrode material in lithium-ion batteries, and recently it has attracted attention for its use in potassium-ion batteries. In this study, the first *in situ* X-ray diffraction characterisation of a K/graphite electrochemical cell is performed. Various graphite intercalation compounds are found, including the stage three KC_{36} and stage one KC_8 compounds, along with the disappearance of the graphite during the potassiation process. These results show new insights on the non-equilibrium states of potassium-ion intercalation into graphite in K/graphite electrochemical cells. © *2017 International Centre for Diffraction Data*.
[doi:10.1017/S0885715617000902]

Key words: potassium-ion, batteries, graphite, negative electrode, *in situ* X-ray diffraction

I. INTRODUCTION

Since its first use as a negative electrode material in the 1980s, graphite holds an important role in battery technology, especially for Li-ion batteries (LIBs) (Tarascon and Armand, 2001). Electrochemical cell voltages exceeding 3.6 V incorporating graphite electrodes and a range of lithium-based transition metal oxide or phosphate positive electrodes are possible. Graphite's theoretical capacity of 372 mAh g^{-1} and low potential against Li^+/Li forms the backbone of LIB technology (Tarascon and Armand, 2001). Furthermore, the abundance and low cost of graphite strengthens its commercial implementation in LIBs (Park *et al*., 2013).

Nevertheless, the use of graphite in LIBs is not without flaws. A number of challenges remain such as the need for more capacity and faster charging times, with future energy storage systems requiring improved safety and higher power output (Tarascon and Armand, 2001). Another significant challenge for lithium-ion technology is the rarity of lithium and the materials associated with the positive electrode (e.g. cobalt) that increase the already high cost of batteries further (Tarascon and Armand, 2001; Palomares *et al*., 2012). The increasing price for lithium and its associated technology is typically considered to be incompatible with the increasing demand for large-scale energy storage coupled with sustainable and clean energy sources such as solar and wind technology (Choi *et al*., 2012). The unstable supply of energy generated from these renewable energy sources requires cheap, efficient, and reliable energy storage systems to ensure the availability of stored energy (Sawicki and Shaw, 2015).

Sodium-ion batteries (SIBs) were proposed as a low-cost alternative for LIBs (Pan *et al*., 2013; Kang *et al*., 2015; Pramudita *et al*., 2017a, 2017b). Sodium's abundance not only results in reduced costs relative to lithium, but also ensures that enough sodium can be acquired to fulfil the demand for large-scale applications (Slater *et al*., 2013). However, SIB development faces a significant hurdle due to the lack of a suitable negative electrode material comparable in performance to graphite in LIBs. Graphite was shown to react unfavourably with Na to form NaC_{64} and produce low capacities of ~35 mAh g^{-1} (Stevens and Dahn, 2001). Thus, researchers have explored the use of alternative forms and formats of carbonaceous materials as negative SIB electrodes, such as hard carbon, which produces capacities of 300 mAh g^{-1} after 120 cycles at C/10 (Ponrouch *et al*., 2013), pitch-cokes that produce 83 mAh g^{-1} after 10 cycles at 7 mA g^{-1} (Thomas *et al*., 1999), or expanded graphite with capacities of 136 mAh g^{-1} after 1000 cycles at 100 mA g^{-1} (Kang *et al*., 2015). These results imply the practical transition from LIBs to SIBs is not straightforward (Wen *et al*., 2014).

Previously, potassium was not considered useful in rechargeable, room temperature, non-aqueous batteries because of its larger size compared with lithium and sodium in light of the unsuccessful intercalation of sodium into graphite (Nobuhara *et al*., 2013; Wen *et al*., 2014; Jian *et al*., 2015; Komaba *et al*., 2015). Using density functional theory (DFT) based calculations, it was shown that Li–graphite intercalation compounds (Li-GICs) and potassium–graphite intercalation compounds (K-GICs) are energetically stable at the high alkali-metal densities of LiC_6 and KC_8, while at the low Na density NaC_{16} is unstable (Nobuhara *et al*., 2013). This is also in agreement with earlier practical work that stabilised the eighth-stage NaC_{64} compound (Ge and Fouletier, 1988). K-GICs are known to form in "stages" based on the number of graphene layers separating the K-intercalated layer, where stage four K-GICs have four graphene layers for every K-intercalated layer, stage three have three, and stage one

a)Author to whom correspondence should be addressed. Electronic mail: vanessa.peterson@ansto.gov.au

has all layers intercalated (Nixon and Parry, 1968). Regarding the implications of the greater mass of potassium relative to lithium and sodium for battery applications, it is noted that the alkali metal weight is not relevant because the pure metal is typically not used due to safety considerations in commercial batteries (Tarascon and Armand, 2001; Komaba *et al*., 2015) and the comparison should therefore be undertaken on the positive electrode material. For example, the mass ratio of the intercalate in P2-type $K_{2/3}CoO_2$ compared with O3-type $LiCoO_2$ is 1.19 (Taniguchi *et al*., 2005). Whilst there are a number of assumptions in this comparison, generally the use of a heavier charge-balancing ion may not significantly affect the total mass of the battery as outlined in recent reviews of potassium-based batteries (Eftekhari *et al*., 2016; Pramudita *et al*., 2017a, 2017b).

The aforementioned studies open up new possibilities for potassium-ion batteries (KIBs). KIBs hold some advantages compared with LIBs, e.g., K being more abundant and thus cheaper (Luo *et al*., 2015). Compared with Na-ions in SIBs, the K-ion has a lower standard reduction potential, suggesting a higher working voltage. Additionally, the fact that graphite can intercalate potassium means that graphite negative electrodes can be used (Luo *et al*., 2015). Several studies have demonstrated the use of graphite negative electrodes in KIBs; however, there still remains a debate on the mechanism of potassium-ion intercalation into graphite (Jian *et al*., 2015; Komaba *et al*., 2015; Luo *et al*., 2015). The first investigation of potassium-ion intercalation in a K/graphite half-cell used *ex situ* X-ray diffraction (XRD) and indicated that insertion occurs through stages of K-GICs, the first being stage three, KC_{36}, detected between 0.3–0.2 V, followed by the stage two KC_{24} phase between 0.2–0.1 V *via* a two-phase reaction (KC_{36} to KC_{24}), before the pure stage one KC_8 was observed near 0.01 V (Jian *et al*., 2015). Shortly after, DFT calculations supported the three stage formation mechanism (Luo *et al*., 2015). However, theoretical calculations and *ex situ* studies often miss important intermediates, thus further studies on the mechanism of potassium-ion intercalation into graphite within batteries are required, ideally using time-resolved techniques. In this study, we report what is to the best of our knowledge the first *in situ* characterisation of potassium-ion intercalation into graphite in KIBs providing new insights on the intercalation mechanism.

II. EXPERIMENTAL

A. Electrochemical characterisation

The graphite electrode for this study was obtained commercially from the MTI corporation. K/graphite coin-type half-cells (CR 2032) were assembled using K metal of ~1 mm thickness and glass-fibre separator soaked in a 1 M potassium hexafluorophosphate (KPF_6) in dimethyl carbonate and ethylene carbonate (1:1 wt%) electrolyte solution. Cells were cycled at 1.5 mA g^{-1} in the voltage range 0.01–2.5 V.

B. Data collection and analysis

In situ synchrotron XRD data were collected from a K/graphite coin-type half-cell (CR 2032) within 3–4 days after cell construction. The coin cell was modified to include 3 mm diameter holes in the casing and a 5 mm diameter hole in the stainless steel spacer. The spacer is a stainless steel plate used to induce pressure inside the coin cell, and it is a standard in coin cell construction. The cells were first discharged to 0.01 V at 5 mA g^{-1}, and then at 6.5 and 8 mA g^{-1}. These procedures were used to ensure sufficient information could be extracted from the limited beamtime available. *In situ* synchrotron XRD data were collected at the Powder Diffraction beamline (Wallwork *et al*., 2007) at the Australian Synchrotron with a wavelength (λ) of 0.70874(2) Å, determined by using the NIST 660b $La^{11}B_6$ standard reference material. Using the multiple battery carousel system developed at the Australian Synchrotron, data for this battery were acquired, amongst batteries used in other research, over 3.4 min every 27.7 min in transmission geometry during charge/discharge (Gu *et al*., 2017).

III. RESULTS AND DISCUSSION

A. Electrochemical characterisation

Figure 1 shows the electrochemical performance of graphite in a typical cell. The first discharge capacity was found to be relatively high, at 521 mAh g^{-1}; however, this decreased to 249 mAh g^{-1} after the first charge. This is typical for carbon-based electrodes and is attributed to the formation of the solid electrolyte interface (SEI) and side reactions occurring during

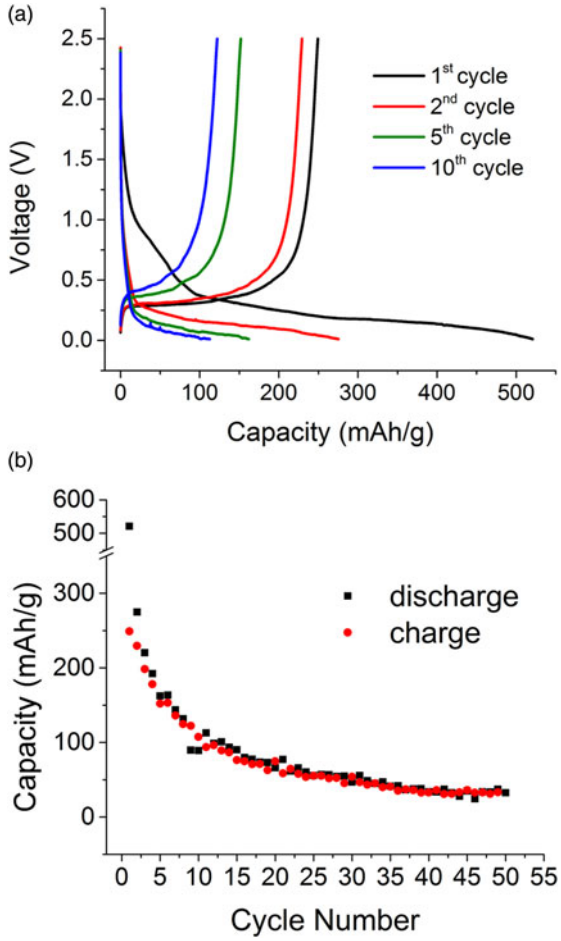

Figure 1. (Colour online) (a) Charge–discharge profile and (b) extended cycling of graphite in a typical potassium half-cell.

https://doi.org/10.1017/S0885715617000902 Published online by Cambridge University Press

the first cycle (Jian *et al*., 2015). By the second discharge, the cell capacity was 274 mAh g^{-1}, in good agreement with previous studies that report a second discharge capacity of 273 mAh g^{-1}, which is close to the theoretical value of 279 mAh g^{-1} for full potassiation, where the phase KC_8 forms (Jian *et al*., 2015). Results for the extended cycling of the cell can be seen in Figure 1(b). This reveals a fade of cell capacity, which is 107 mAh g^{-1} after the 10th cycle, 73 mAh g^{-1} after the 20th cycle, and only 34 mAh g^{-1} after the 50th cycle. This behaviour, though not as severe, has been noted previously, with steady capacity fade from 197 to 100 mAh g^{-1} by the 50th cycle (Jian *et al*., 2015). Capacity fade is thought to arise from the large volume expansion of graphite during potassium insertion/extraction and/or a less stable and lower conducting SEI compared with the Li counterpart (Jian *et al*., 2015; Pramudita *et al*., 2017a, 2017b). The electrochemical performance can be improved by using an electrolyte composed of 0.5 M KPF_6 in ethylene carbonate:diethyl carbonate or 1 M potassium bis(fluorosulfonyl)imide (KFSI) in ethylene carbonate:diethyl carbonate, where a capacity above 200 mAh g^{-1} can be maintained until the 50th cycle (Komaba *et al*., 2015).

B. *In situ* X-ray diffraction

In situ XRD was performed for the first time on a potassium-ion cell to understand the mechanism for K^+ insertion into graphite. Figure 2 shows the XRD data for the cell at the beginning of the insertion process. All reflections aside from three very small reflections at ~11.9°, 12.4°, and 14.3° 2θ could be indexed to phases of graphite (Hassel and Mark, 1924) with space group $P6_3/mmc$ and lattice parameters $a = 2.4630(8)$ Å and $c = 6.7182(2)$ Å, and the Cu phase of the current collector.

Figure 3 shows a contour plot of the *in situ* XRD data highlighting graphite reflections during the cell discharge. Detector issues at ~550 min resulted in a drop in intensity and data in this region were removed. Small fluctuations in both 2θ and intensity of all reflections (particularly evident for the stronger reflections at higher scattering angles) were noted, possibly arising from the irreproducibility in sample position between repeat rotations of the sample environment carousel. Nevertheless, the *in situ* data contain phase information that gives insight into the potassiation process. The strongest graphite reflection, 002, decreases in intensity as the discharge proceeds until it disappears at ~0.25 V. Similarly, the graphite 100 reflection decreases in intensity during discharge, but does not completely disappear. The graphite 101 and weaker 004 reflections also decrease in intensity and disappear at ~0.2–0.3 V. The 110 reflection decreases in intensity and also shows a subtle shift to a lower 2θ value by ~0.1°. The last two identifiable reflections, the graphite 112 and 300 reflections, also steadily decrease in intensity during discharge and disappear at ~0.2 V.

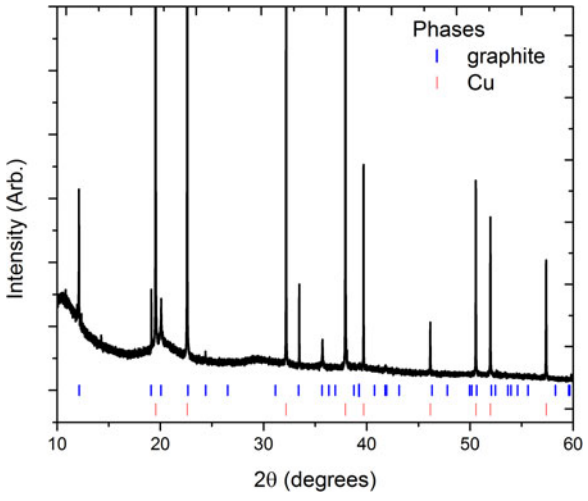

Figure 2. (Colour online) XRD data for the uncycled cell. Vertical lines are Bragg reflection markers for the graphite and copper current collector.

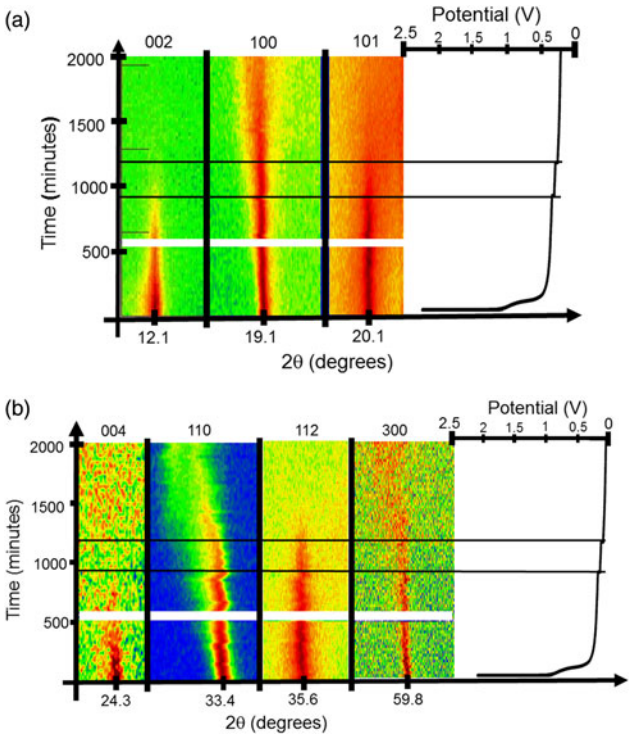

Figure 3. (Colour online) Selected 2θ regions of the *in situ* synchrotron XRD data highlighting the evolution of reflections of interest from graphite, the (a) graphite 002, 100, and 101, and (b) 004, 110, 112, and 300 reflections. The area without data is a consequence of detector issues. The black horizontal lines show times where the current increased, first one to 6.5 mA g^{-1} and then to 8 mA g^{-1}.

Figures 4(a) and 4(b) show the phase evolution of new reflections appearing during graphite potassiation occurring during the cell discharge. Previous work investigating the gas-phase (Nishitani *et al*., 1983) and chemical (Mizutani *et al*., 1996) potassiation of graphite revealed a complex staging process of K-GICs consisting of up to seven phases, each found to have predominantly *P6/mmm* symmetry (Böhm *et al*., 1996). The dominant features of XRD data for these potassiated phases are the [00*l*] basal-plane reflections and we consider our data with respect to reflections associated with the stacking *c*-axis of these *P6/mmm* phases in which higher order reflections follow the expected *d*001/*l* spacing.

Following the decrease of intensity of the graphite 002 reflection, a new reflection at 2θ = 14.3° appears at ~0.62 V. The *d*-spacing of this reflection [$d = 2.853(5)$ Å] is near to the 004 reflection of the "stage three" KC_{36} phase

https://doi.org/10.1017/S0885715617000902 Published online by Cambridge University Press

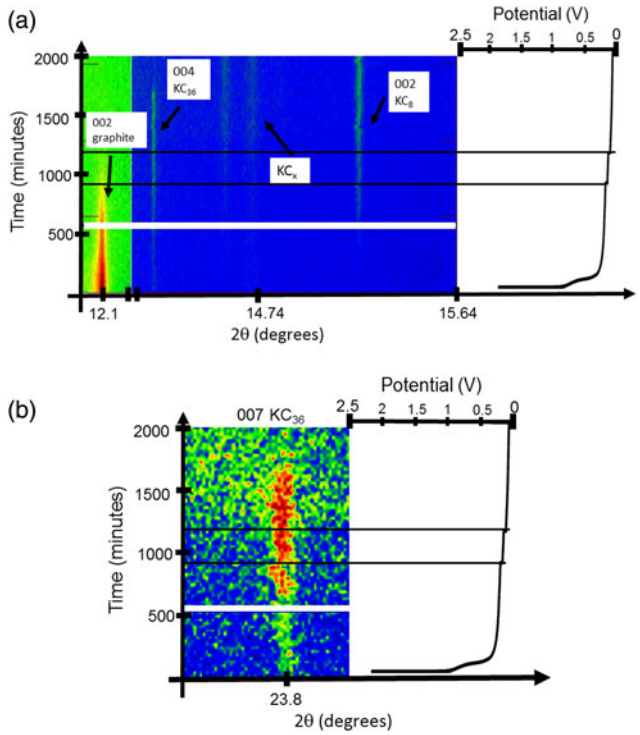

Figure 4. (Colour online) Selected 2θ regions of *in situ* synchrotron XRD data highlighting the evolution of the graphite 002 reflections and new reflections associated with the potassiation of graphite, (a) the graphite 002, KC_{36} 004, KC_x, KC_8 002, and (b) KC_{36} 007 reflections. The area without data is a consequence of detector issues. The black horizontal lines show times where the current increased, first one to 6.5 mA g^{-1} and then to 8 mA g^{-1}.

previously observed at $d \approx 3.0$ Å (Jian *et al.*, 2015), and the corresponding KC_{36} 007 reflection can be seen appearing also at ~0.62 V. At this stage in the discharge the graphite 002 reflection is still present. Interestingly, at ~0.3 V we see the appearance of a reflection at $2\theta = 15.2°$ [$d = 2.680(2)$ Å] near to the 002 reflection of the "stage one" potassiated graphite phase, KC_8 at $d \approx 2.7$ Å, at 0.01 V (Jian *et al.*, 2015), at a much higher potential than previously reported using *ex situ* characterisation. The graphite 002 reflection disappears at ~0.25 V, where the KC_{36} and KC_8 reflections remain. At ~0.2 V new reflections appear at $2\theta = 14.6°$ and 14.7° [$d =$ 2.790(1) and 2.766(1) Å], which do not correspond to higher order 00*l* reflections for any previously reported phases. Further, the co-appearance of these two reflections suggests they arise from the same phase, denoted the unknown KC_x phase. Satellite reflections due to modulation effects in potassium-intercalated graphite have been observed at low potassium concentrations using XRD (Zabel, 1981; Purewal, 2010), and the very low reflection intensity and close appearance of these reflections is consistent with this. Regardless, the relatively-small Q range over which these powder data were collected limits further analysis of these reflections, which will be the subject of future work. Close to 0.05 V the KC_{36} phase disappears. Finally, at the 0.01 V discharged state, the potassiated graphite comprises the fully potassiated KC_8 phase alongside the two reflections of the KC_x phase. The reflection *d*-spacing and their phase association is summarised in Table I.

In situ data clearly show the formation of the KC_8 phase earlier in the discharge process than previously observed in *ex*

TABLE I. Potassiated graphite reflections observed in this study and in the previous *ex situ* study (Mizutani *et al.*, 1996; Jian *et al.*, 2015).

Reflections (this study)			Reflections (Jian *et al.*, 2015)
2θ (°)	*d*-spacing (Å)	Phase	*d*-spacing (Å)
12.1(2)	3.357(2)	Graphite 002	
14.3(3)	2.853(5)	KC_{36} 004	~3.0
		KC_{24} 003	~2.9
14.6(4)	2.790(3)	KC_x	
14.7(4)	2.766(3)	KC_x	
15.2(3)	2.680(2)	KC_8 002	~2.7
23.8(5)	1.721(7)	KC_{36} 007	

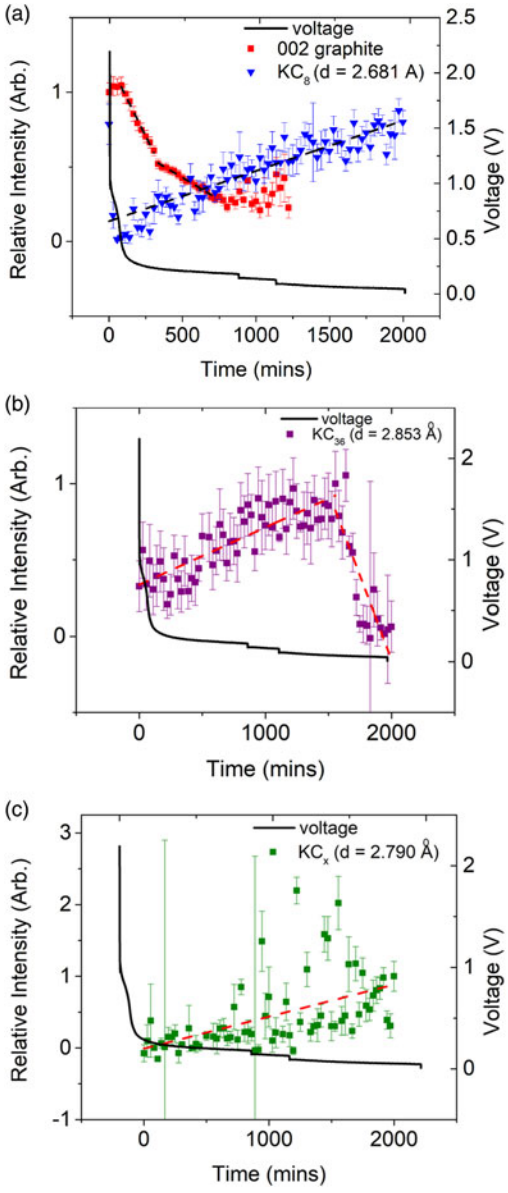

Figure 5. (Colour online) Results from single peak fitting of the (a) graphite 002 ($R^2 = 0.98639$ and 0.98121 sequentially) and KC_8 002 ($R^2 = 0.92657$), (b) KC_{36} 004 ($R^2 = 0.67671$ and 0.69858 sequentially), and (c) unknown KC_x phase ($R^2 = 0.4259$) reflections plotted with the voltage profile. Dashed line shows the linear fit of the reflection intensity variation with time. Data in (a) and (b) are presented as fractional change from the maximum value, which was 85.45 counts for the graphite 002 reflection, 10.47 counts for the KC_8 reflection, and 3.36 counts for the reflection in (b).

https://doi.org/10.1017/S0885715617000902 Published online by Cambridge University Press

TABLE II. Rate of change of reflection intensities obtained from the linear fit to data shown in Figure 5.

Phase reflection	Rate of increase (counts min^{-1})	Rate of decrease (counts min^{-1})
Graphite 002		0.198(2) and 0.0592(2)
KC_{36} 004	0.0377(3)	0.219(4)
KC_x	0.0447(8)	–
KC_8 002	0.0338(1)	–

situ XRD experiments (Jian *et al*., 2015), and that this phase co-exists alongside the graphite and KC_{36} phases. Our measurements capture the non-equilibrium states of the reaction as it proceeds, and this may in part explain the presence of different stages of K-GICs at the end of the discharge cycle where pure or mostly pure KC_8 is expected. Further, throughout the discharge process a change in the background, especially at the lower 2θ range, was observed. This suggests that additional processes involving non-crystalline or disordered phases are likely present. In contrast to the intercalation process of Li into graphite, the solid solution processes that are strongly observed during the lithiation of graphite have not been observed for the corresponding potassiation (Senyshyn *et al*., 2013; Sharma and Peterson, 2013).

The time evolution of the individual K-GIC reflections was examined using single-peak fitting and results are shown in Figure 5 and Table II. The rate of change of the intensity was obtained by linear fitting of the data. The graphite 002 reflection shows a two-step process, gradually decreasing in relative intensity at $-0.198(2)$ counts min^{-1} to 0.25 V, then more slowly at $-0.0592(2)$ counts min^{-1} which corresponds to the appearance of the KC_8 phase before disappearing. The stage one KC_8 002 reflection intensity steadily increases at 0.0338(1) counts min^{-1}, slower than the decay in the graphite reflection.

Figures 5(b) and 5(c) show the time evolution of the KC_{36} 004 reflection and the reflection for the unknown KC_x reflection at $2\theta = 14.6°$. The results of these fits are less reliable due to their relatively weaker overall intensities. The KC_{36} 004 reflection intensity grows at 0.0377(3) counts min^{-1} reaching a maximum at ~0.04 V before decreasing rapidly at a rate of $-0.219(4)$ counts min^{-1} and disappearing. This suggests that the formation of the KC_{36} phase is relatively slow, but its transformation to a higher potassiated phase is much faster. Lastly, the formation of the unknown KC_x phase is relatively slow, growing at 0.0447(8) counts min^{-1}.

While a more detailed study is clearly warranted to fully determine and characterise the potassium intercalation phases of graphite, it can be clearly seen that the mechanism observed in this *in situ* study bears some significant differences compared to the previous *ex situ* studies. In particular, an earlier (in terms of potential) formation of the different stages of potassium intercalation compounds and a different order of appearance than previously observed (Jian *et al*., 2015; Luo *et al*., 2015) was found.

IV. CONCLUSION

The first *in situ* XRD measurement of potassium-ion intercalation into graphite in a potassium-ion battery was undertaken. The K/graphite electrochemical cell produced a reversible capacity of 249 mAh g^{-1} which is comparable with the literature; however, it does not retain its capacity over a long period of cycling, also as expected. The *in situ* XRD study shows the transformation of the graphite phase to various potassium intercalation compounds. The sequence of the formation of various potassium intercalation phases is found to occur at different potentials than noted in previous work using *ex situ* XRD. Notably, we find the formation of stage three KC_8 at the higher potential of 0.3 V. Thus, this study reveals the importance of studying *in situ* the formation of these phases in order to examine the non-equilibrium states of potassium-ion intercalation into graphite in potassium-ion batteries, promoting a deeper understanding of electrode function to realise commercial potassium-ion batteries.

ACKNOWLEDGEMENTS

James C. Pramudita would like to thank UNSW/ANSTO and AINSE for PhD scholarships. Neeraj Sharma would like to thank the Australian Research Council for support (DE160100237/DP170100269). Part of this research was undertaken on the Powder Diffraction beamline at the Australian Synchrotron, Victoria, Australia.

Böhm, M. C., Schulte, J., and Schlögl, R. (**1996**). "Electronic structure of potassium graphite compounds," Phys. Status Solidi. **131**, 131–144.

Choi, N.-S., Chen, Z., Freunberger, S. A., Ji, X., Sun, Y.-K., Amine, K., and Bruce, P. G. (**2012**). "Challenges facing lithium batteries and electrical double-layer capacitors," Angew. Chem. Int. Ed. **51**, 9994–10024.

Eftekhari, A., Jian, Z., and Ji, X. (**2016**). "Potassium secondary batteries," ACS Appl. Mater. Interfaces **9**, 4404–4419.

Ge, P. and Fouletier, M. (**1988**). "Electrochemical intercalation of sodium in graphite," Solid State Ion. **28**, 1172–1175.

Gu, Q., Kimpton, J. A., Brand, H. E. A., Wang, Z., and Chou, S. (**2017**). "Solving key challenges in battery research using *in situ* synchrotron and neutron techniques," Adv. Energy Mater. doi: 10.1002/aenm.201602831.

Hassel, O. and Mark, H. (**1924**). "Über die Kristallstruktur des Graphits," Z. Phys. A Hadrons Nucl. **25**, 317–337.

Jian, Z., Luo, W., and Ji, X. (**2015**). "Carbon electrodes for K-ion batteries," J. Am. Chem. Soc. **137**, 11566–11569.

Kang, H., Liu, Y., Cao, K., Zhao, Y., Jiao, L., Wang, Y., and Yuan, H. (**2015**). "Update on anode materials for Na-ion batteries," J. Mat. Chem. A **3**, 17899–17913.

Komaba, S., Hasegawa, T., Dahbi, M., and Kubota, K. (**2015**). "Potassium intercalation into graphite to realize high-voltage/high-power potassium-ion batteries and potassium-ion capacitors," Electrochem. Commun. **60**, 172–175.

Luo, W., Wan, J., Ozdemir, B., Bao, W., Chen, Y., Dai, J., and Hu, L. (**2015**). "Potassium ion batteries with graphitic materials," Nano Lett. **15**, 7671–7677.

Mizutani, Y., Ihara, E., Abe, T., Asano, M., Harada, T., Ogumi, Z., and Inaba, M. (**1996**). Preparation of alkali metal graphite intercalation compounds in organic solvents," J. Phys. Chem. Solids **57**, 799–803.

Nishitani, R., Uno, Y., and Suematsu, H. (**1983**). "*In situ* observation of staging in potassium-graphite intercalation compounds," Phys. Rev. B. **27**, 6572–6575.

Nixon, D. E., and Parry, G. S. (**1968**). "Formation and structure of the potassium graphites," J. Phys. D: Appl. Phys. **1**, 291.

Nobuhara, K., Nakayama, H., Nose, M., Nakanishi, S., and Iba, H. (**2013**). "First-principles study of alkali metal-graphite intercalation compounds," J. Power Sources **243**, 585–587.

Palomares, V., Serras, P., Villaluenga, I., Hueso, K. B., Carretero-Gonzalez, J., and Rojo, T. (**2012**). "Na-ion batteries, recent advances and present challenges to become low cost energy storage systems," Energy Environ. Sci. **5**, 5884–5901.

Pan, H., Hu, Y.-S., and Chen, L. (**2013**). "Room-temperature stationary sodium-ion batteries for large-scale electric energy storage," Energy Environ. Sci. **6**, 2338–2360.

Park, T.-H., Yeo, J.-S., Seo, M.-H., Miyawaki, J., Mochida, I., and Yoon, S.-H. (**2013**). "Enhancing the rate performance of graphite anodes through addition of natural graphite/carbon nanofibers in lithium-ion batteries," Electrochim. Acta **93**, 236–240.

Ponrouch, A., Goñi, A. R., and Palacín, M. R. (**2013**). "High capacity hard carbon anodes for sodium ion batteries in additive free electrolyte," Electrochem. Commun. **27**, 85–88.

Pramudita, J. C., Rawal, A., Choucair, M., Pontiroli, D., Magnani, G., Gaboardi, M., and Sharma, N. (**2017a**). "Mechanisms of sodium insertion/extraction on the surface of defective graphenes," ACS Appl. Mater. Interfaces **9**, 431–438.

Pramudita, J. C., Sehrawat, D., Goonetilleke, D., and Sharma, N. (**2017b**). "an initial review of the status of electrode materials for potassium-ion batteries," Adv. Energy Mater. doi: 10.1002/aenm.201602911.

Purewal, J. (**2010**). Hydrogen adsorption by alkali metal graphite intercalation compounds. PhD Dissertation, California Institute of Technology.

Sawicki, M. and Shaw, L. L. (**2015**). "Advances and challenges of sodium ion batteries as post lithium ion batteries," RSC Adv. **5**, 53129–53154.

Senyshyn, A., Dolotko, O., Mühlbauer, M. J., Nikolowski, K., Fuess, H., and Ehrenberg, H. (**2013**). "lithium intercalation into graphitic carbons revisited: experimental evidence for twisted bilayer behavior," J. Electrochem. Soc. **160**, A3198–A3205.

Sharma, N. and Peterson, V. K. (**2013**). "Overcharging a lithium-ion battery: effect on the LixC6 negative electrode determined by *in situ* neutron diffraction," J. Power Sources **244**, 695–701.

Slater, M. D., Kim, D., Lee, E., and Johnson, C. S. (**2013**). "Sodium-ion batteries," Adv. Funct. Mater. **23**, 947–958.

Stevens, D. A. and Dahn, J. R. (**2001**). "The mechanisms of lithium and sodium insertion in carbon materials," J. Electrochem. Soc. **148**, A803–A811.

Taniguchi, H., Ebina, Y., Takada, K., and Sasaki, T. (**2005**). "Synthesis and soft-chemical reactivity of layered potassium cobalt oxide," Solid State Ion. **176**, 2367–2370.

Tarascon, J. M. and Armand, M. (**2001**). "Issues and challenges facing rechargeable lithium batteries," Nature **414**, 359–367.

Thomas, P., Ghanbaja, J., and Billaud, D. (**1999**). "Electrochemical insertion of sodium in pitch-based carbon fibres in comparison with graphite in NaClO4–ethylene carbonate electrolyte," Electrochim. Acta **45**, 423–430.

Wallwork, K. S., Kennedy, B. J., and Wang, D. (**2007**). "The high resolution powder diffraction beamline for the australian synchrotron," AIP Conf. Proc. **879**, 879–882.

Wen, Y., He, K., Zhu, Y., Han, F., Xu, Y., Matsuda, I., and Wang, C. (**2014**). "Expanded graphite as superior anode for sodium-ion batteries," Nat. Commun. **5**, 4033.

Zabel, H. (**1981**). *Ordering in 2 dimensions* (North Holland Publishing, Amsterdam).

https://doi.org/10.1017/S0885715617000902 Published online by Cambridge University Press